Analysis of Shoe Friction During Sliding Against Floor Material: Role of Fluid Contaminant

Caitlin T. Moore

Pradeep L. Menezes

Michael R. Lovell

Kurt E. Beschorner[1]

e-mail: beschorn@uwm.edu

Department of Industrial Engineering,
University of Wisconsin-Milwaukee,
Milwaukee, WI 53201

Understanding the tribological interactions between shoe and floor materials is important in order to enhance shoe and floor design and to prevent slip and fall accidents during walking. In the present investigation, experiments were conducted using a custom developed pin-on-disk type tribometer to understand the influence of boundary and hydrodynamic properties on the shoe-floor materials' coefficient of friction. Specifically, polyurethane shoe material was slid against vinyl floor material in the presence of varying lubricants (i.e., water, detergent, three diluted glycerol concentrations, and canola oil). The experiments were conducted for a range of biologically relevant sliding velocities from 0.05 m sec^{-1} to 1.0 m sec^{-1} at a contact pressure of 266.1 kPa under ambient conditions. The fluid chemical composition appeared to affect the boundary friction coefficient with longer-chain molecules resulting in a decreased coefficient of friction. As fluid viscosity increased, the rate of coefficient of friction decay increased with respect to increasing fluid entrainment velocity, suggesting less material contact and increased film thickness. The nondimensional film thickness under all conditions was calculated and the nondimensional film thickness consistently increased with increased viscosity and speed. Additionally, the effect of functionally achievable variations in polyurethane shoe roughness on the coefficient of friction was examined and found to have no statistically significant effect on boundary or hydrodynamic contributions to the coefficient of friction. [DOI: 10.1115/1.4007346]

Keywords: friction, viscosity, lubricants

1 Introduction

Fall accidents represent a serious social and economic burden. According to the Liberty Mutual Workplace Safety Index (WSI), in 2007, occupational fall accidents that occurred on the same level cost approximately $\$7.7 \times 10^9$ in the United States alone [1]. Among various fall accidents, 40–50% of fall related injuries were induced by slipping [2], with an estimated 24% being attributed to improper shoe material and 50% to improper floor material [3]. According to the Bureau of Labor Statistics (BLS), in 2008, accidents due to falls on the same level resulted in a median of 10 days away from work for the employee to recover [4].

Slip initiation occurs when the amount of required friction for walking exceeds the available friction at the shoe-floor interface [5,6]. The average required coefficient of friction (RCOF) during normal gait on a level surface has been reported between 0.17 and 0.22 [5,7–10]. The available friction is affected by the shoe and floor material properties [11–13], surface topography [14–17], tread pattern [18–20], fluid lubricant [11,13,21,22] and operating conditions [21,22] and have been shown to relate to wear [12,17].

Among the many factors that are known to affect shoe-floor-fluid friction, the tribological interaction of the shoe-floor-fluid interface has typically been discussed only with regard to the hydrodynamic effects of the fluid. These factors include the squeeze-film effect [23], the wedge-term [24], and shoe material deformation due to elastohydrodynamic lubrication (EHL) [25]. In regard to fluid pressure effects, the shoe-floor-liquid contaminant coefficient of friction typically decreases as speed increases, which is consistent with the Stribeck effect and can be described by three lubrication regions: boundary lubrication, mixed lubrication, and hydrodynamic lubrication [21,26]. Boundary lubrication results in the greatest material asperity contact and, therefore, the highest coefficient of friction. Under boundary lubrication, the molecular structure of the lubricant affects the available friction with long chains and polar molecules providing the best lubrication [27]. As the sliding speed increases, the hydrodynamic pressure increases and separates some of the shoe and floor asperities, which ultimately reduces the friction coefficient [24,25]. Factors that affect the hydrodynamics between shoe and floor surfaces include fluid viscosity, sliding speed, shoe shape and orientation, normal force, and surface topography [24,26]. In general, rougher surfaces offer void volumes for the liquid contaminant to settle into without reducing the material asperities' ability to maintain contact. In the literature, researchers have reported that the floor material roughness significantly affects the coefficient of friction [14–16,28]. Chang [14] showed that floors with higher asperity peaks and an increased void volume resulted in an increased friction coefficient. However, much less research has been done on the effect of shoe roughness on the shoe-floor coefficient of friction. Hence, in this study, attempts were made to determine the influence of shoe roughness and fluid contaminant on the shoe-floor-fluid friction.

An improved understanding of shoe-floor-contaminant friction mechanisms also aids the development of shoe-floor-fluid tribological models that are currently being developed. Progress has been made in modeling shoe-floor-fluid friction under mixed lubrication by taking into account the hydrodynamic effect of the fluid [26]. This model showed good agreement between the model output and experimental data, however, it did not model boundary lubrication effects nor did it evaluate the effects of shoe roughness on shoe-floor-fluid friction. Identifying and examining factors which affect boundary lubrication will help to develop more advanced shoe-floor-contaminant friction models and will lead to the development of more slip resistant shoe and floor designs.

In this context, the goal of the present research is to examine the effect of lubricant properties on shoe-floor-fluid friction while

[1]Corresponding author.

Contributed by the Tribology Division of ASME for publication in the JOURNAL OF TRIBOLOGY. Manuscript received March 24, 2011; final manuscript received June 23, 2012; published online September 4, 2012. Assoc. Editor: Michael D. Bryant.

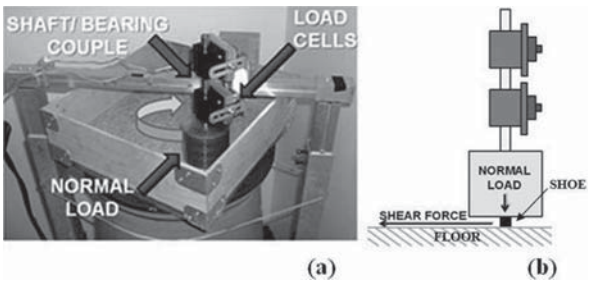

Fig. 1 Custom pin-on-disk tribometer used to measure the shoe-floor-contaminant coefficient of friction: (*a*) photograph, and (*b*) schematic showing floor material (disk), shoe material (pin), and the direction of the shear and normal forces used to calculate the coefficient of friction

considering both the boundary lubrication and hydrodynamic effects. As a secondary goal, the effect of the achievable variation in shoe roughness was examined.

2 Methods

Experiments were conducted using a pin-on-disk type tribometer, the photograph and schematic views of which are shown in Figs. 1(*a*) and 1(*b*), respectively. The pin-on-disk type tribometer was custom developed by instrumenting a rate table (disk) on which the floor material is mounted. A normal load is applied to the shaft directly above the shoe material (pin). When the rate table rotates relative to the fixed shoe material the frictional (or shear) force is recorded by load cells. The coefficient of friction was measured as the ratio between the measured shear (frictional) force and the applied normal force.

A pin-on-disk tribometer was used in this study because of its flexibility to easily modify testing conditions and to fundamentally understand the interactions of the shoe and floor surfaces. It is expected that the shoe tread pattern and loading conditions that exist during actual slipping accidents may affect the exact coefficient of friction measurements. Yet, because previous research by one of the present authors [21] has shown a similar Stribeck effect with entire shoes, it is anticipated that the general trends that are identified in this study are applicable to whole-shoe testing. Using the pin-on-disk type apparatus, the sliding speed can be varied over a range of speeds that are relevant to walking. Previous publications have described the requirements for biomechanically relevant, 'biofidelic,' slip resistance testing and recommended a sliding velocity at the shoe-floor interface between 0-1.0 m sec^{-1} [22]. In the present study, experiments were conducted for 11 defined, biologically relevant sliding speeds, namely 0.05, 0.1, 0.2, 0.3, 0.4, 0.5, 0.6, 0.7, 0.8, 0.9, and 1.0 m sec^{-1}. In addition, all tests were carried out for a constant normal load of 20.9 N in ambient conditions, resulting in a contact pressure of approximately 266.1 kPa. The normal load was selected in order to achieve a contact pressure between 200 and 1000 kPa, which has been identified as a biomechanically-relevant range of pressures [22]. In order to isolate the boundary lubrication and wedge term effects specific to the shoe and floor materials rather than the performance of a whole shoe design against a floor surface, other biologically relevant parameters (i.e., shoe angle, tread, and normal force build-up rate) were not incorporated into the experimental design. A typical variation in the coefficient of friction values recorded over a 10 s period is presented in Fig. 2. As part of the protocol, five experiments were recorded for each testing condition. The order of each set of experiments was randomized.

In the experiments presented here, the materials and contaminants relevant to shoe-floor friction were examined. The pins were made of untreaded polyurethane and the counterpart, the floor material, was made of commercially available vinyl tile. The pins were 10 mm in diameter with a reduced radius of curvature of approximately 23.3 μm. The floor material for all experiments was standard 305 mm $\times$ 305 mm, 35 mm thick vinyl floor tiles with a track radius of 80 mm. The surface roughness parameter, the RMS of roughness (R_q), of the shoe and floor materials was measured using a 2D contact type stylus profilometer with a cutoff filter length of 0.8 mm. A single floor material was used for all testing with a roughness value of $R_q = 1.34 \pm 0.2\ \mu$m. The roughness of the polyurethane shoe material was controlled by abrading the shoe material with 220 grit silicon carbide paper for each experiment, resulting in a roughness of approximately 8.2 μm. The fluid contaminants examined are water, 1.5% detergent, a 25% water-75% glycerol concentration, a 50% water-50% glycerol concentration, a 75% water-25% glycerol concentration, and canola oil with corresponding viscosities of 0.52 cP, 1.8 cP, 1.9 cP, 5.54 cP, 41 cP, and 74.6 cP, respectively. The viscosity of the fluids was measured at ambient conditions (approximately 20–25 °C) using a viscometer. The detergent-water concentration was selected to follow the manufacturer's instructions of approximately 1.5% detergent for normal cleaning. Canola oil was selected since it is commonly present in a restaurant setting. Glycerol was chosen because the fluid concentrations and viscosity can be easily varied to study the viscosity effects.

In another set of experiments, the ability to vary the frictional effects by varying the shoe roughness was explored. To vary the

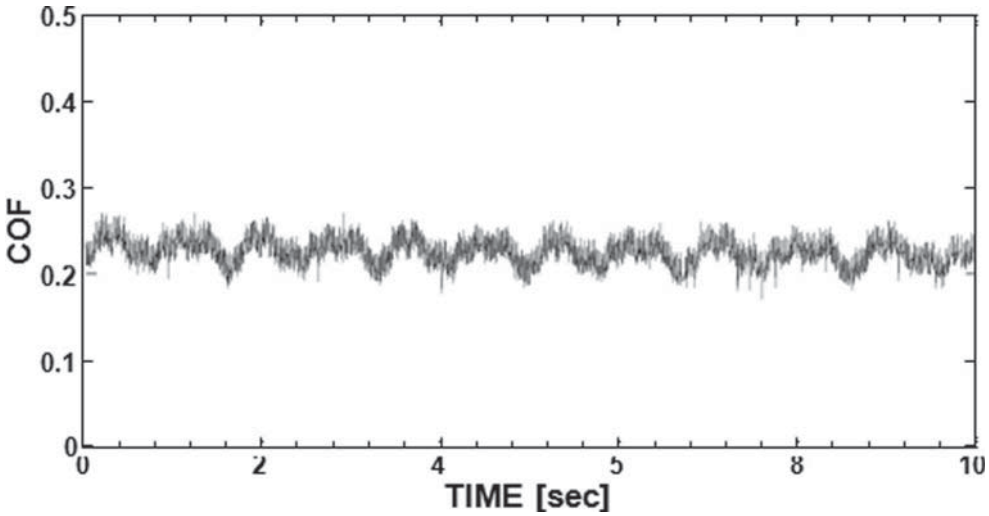

Fig. 2 Typical time-history of the coefficient of friction

polyurethane shoe roughness, the shoe material was abraded with varying grades of silicon carbide paper, which resulted in a limited range of achievable variation in the RMS roughness, 9.3 μm, 8.2 μm, and 7.3 μm, corresponding to 100 grit, 220 grit, and 400 grit silicon carbide paper, respectively. For these experiments, three combinations of glycerol and water, namely, 25% water-75% glycerol, 50% water-50% glycerol, and 75% water-25% glycerol that were used in the previously described set of experiments were applied to the shoe-floor contact.

Consistent with previous research, lubricated shoe-floor friction decayed with increasing speed, following the Stribeck effect [21,26]. An exponential decay fit was used to quantify the change (resistance to decay) in the coefficient of friction with increasing speed. A regression analysis was performed using the following equation calculating variables relevant to quantifying boundary lubrication friction and friction decay with speed

$$\mathrm{COF} = \mathrm{COF}_{\mathrm{asymptote}} + (\mathrm{COF}_{\mathrm{BL}} - \mathrm{COF}_{\mathrm{asymptote}})e^{-v/\tau_{\mathrm{hydro}}} \quad (1)$$

Equation (1) tracks the change in the coefficient of friction with speed and quantifies the boundary lubrication and hydrodynamic effects. Here, the $\mathrm{COF}_{\mathrm{BL}}$ is indicative of the coefficient of friction under boundary lubrication, which occurs at very low speeds before the hydrodynamic effects cause a dramatic decrease in friction, and was calculated for the coefficient of friction value as the velocity approaches zero. The variable τ_{hydro} represents the resistance to decay of the coefficient of friction due to fluid pressure or hydrodynamic lubrication effects, which cause the coefficient of friction to decrease. Here, τ_{hydro} is a measure most closely related to the hydrodynamic fluid effects, which causes the coefficient of friction to decay under the mixed-lubrication regime. As the velocity increases to high sliding speeds, the coefficient of friction approaches an asymptote, which is quantified by the variable $\mathrm{COF}_{\mathrm{asymptote}}$.

An optimization method, the Nelder-Mead simplex method [29], was used to fit the preceding model, i.e., Eq. (1), to the collected coefficient of friction data. Figure 3 shows an example dataset fit with the regression equation (Eq. (1)), resulting in a calculated boundary coefficient of friction ($\mathrm{COF}_{\mathrm{BL}}$) of 0.83, a calculated hydrodynamic effect (τ_{hydro}) of 0.18, and an asymptote ($\mathrm{COF}_{\mathrm{asymptote}}$) of 0.16. The Nelder-Mead simplex method is a direct search method of nonlinear unconstrained optimization and was applied to minimize the Euclidean distance between the predictive exponential function and the collected coefficient of friction data, resulting in a best fit equation [29,30]. The $\mathrm{COF}_{\mathrm{asymptote}}$ and $\mathrm{COF}_{\mathrm{BL}}$ were bounded using MATLAB [31] so that the resulting best fit does not include coefficient of friction values less than zero.

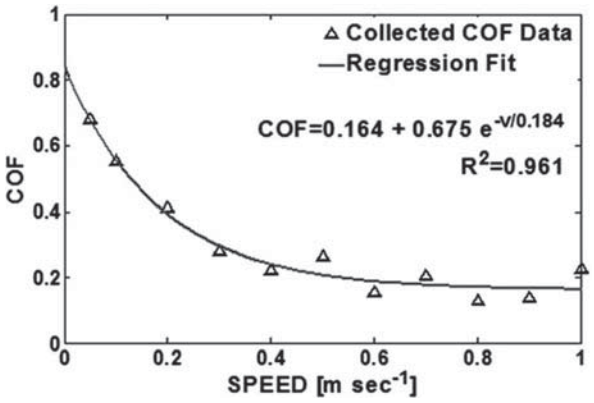

Fig. 3 Variation of the coefficient of friction with speed (triangles) for 25% glycerol-75% water lubrication and 8.2 μm shoe roughness; the solid line represents the exponential regression fit. The values obtained for the variables of Eq. (1) are $\mathrm{COF}_{\mathrm{BL}} = 0.839$, $\tau_{\mathrm{hydro}} = 0.184$, and $\mathrm{COF}_{\mathrm{asymptote}} = 0.164$.

In addition to quantifying the boundary and hydrodynamic effects of the empirical data, the theoretical nondimensional film thickness of each shoe-floor-contaminant combination was calculated. Based on maps of the lubrication regimes developed by Esfahanian and Hamrock [32], the shoe-floor-lubricant contact was identified to function under the isoviscous-elastic regime, also known as soft-EHL. In the isoviscous-elastic regime, the fluid pressures are relatively low and elastic deformation of material relative to the film thickness is relatively high [33]. This regime is commonly encountered in scenarios such as seals and tires [33]. Hamrock and Dowson developed the nondimensional film thickness equation under soft-EHL by least-square fitting data based on 17 soft-EHL conditions [33]. Under soft-EHL contact, the nondimensional film thickness is calculated from the following equation [33]

$$\tilde{H}_{e,\min} = 7.43U^{0.65}W^{-0.21}\left(1 - 0.85e^{-0.31k}\right) \quad (2)$$

where

$$\tilde{H}_{e,\min} = \frac{\tilde{h}_{\min}}{R'}$$

$$U = \frac{\eta v}{E'R'}$$

$$W = \frac{w}{E'R'}$$

The parameters (velocity (v), reduced radius of curvature (R'), viscosity (η), effective elastic modulus (E'), and normal load (w)) which were used to calculate the film thickness were measured or calculated. The velocity, viscosity, and normal load were measured as testing parameters. The effective elastic modulus was assumed to be approximately equivalent to the elastic modulus of the much softer material, polyurethane, and measured to be approximately 2.0 MPa [26]. Table 1 summarizes all of the relevant parameters used to calculate the nondimensional film thickness. The reduced radius of curvature was calculated by measuring the 2D surface profile of the shoe pin and fitting a second-order polynomial, Eq. (3) [26], to the profile of the shoe material to determine the curvature of the material

$$h(r) = B * r^2 \quad (3)$$

The reduced radius of curvature is then calculated from Eq. (4). Figure 4 shows an example of a surface profile fit with the second-order polynomial. The regression variable indicative of curvature B was determined by regression fitting

$$R' = \frac{1}{2 * B} \quad (4)$$

The assumption that the shoe sample was symmetric was made based on similar profile scans in perpendicular directions, resulting in $k = 1$. The ratio of the film thickness to roughness (λ) is related to the transition between the boundary lubrication, mixed lubrication, and full-film lubrication. The ratio relates to the asperity contact available. When λ is less than 1, the contact is defined to be in the boundary lubrication regime. When λ is between 1 and 3, the contact is defined to be within the mixed lubrication

Table 1 Parameters used to calculate non-dimensional film thickness

Fluid viscosity, η	0.52, 1.8, 1.9, 5.54, 41, 74.6 cP
Velocity, v	0.05, 0.1, 0.2, 0.3, 0.4, 0.5, 0.6, 0.7, 0.8, 0.9, 1.0 m sec^{-1}
Effective elastic modulus, E'	2.0 MPa
Normal load, w	20.9 N
Reduced radius of curvature, R'	23.3 μm

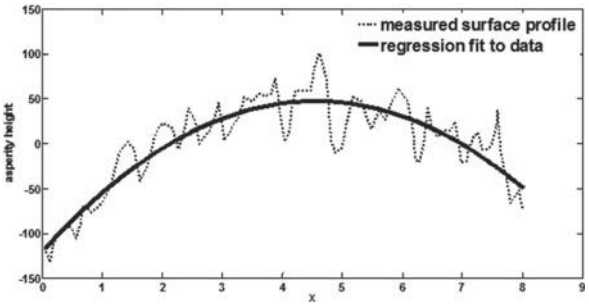

Fig. 4 Example of a surface profile fit with a second-order polynomial to calculate the reduced radius of curvature (R'); the dotted line shows the measured surface profile and the solid line is the second-order polynomial regression fit to the data

regime. When λ is greater than 3, the contact is defined to be in the full-film lubrication regime. The variable is calculated from the following equation [33]

$$\lambda = \frac{\tilde{H}_{e,\min} * R'}{\sigma^*} \tag{5}$$

2.1 Statistical Analysis. Analysis of variance (ANOVA) analyses were conducted to determine the effects of the fluid composition and fluid viscosity on the lubrication parameters: COF_{BL}, τ_{hydro}, and $COF_{asymptote}$. In the study, the fluid composition was treated as a nominal variable, while the fluid viscosity was treated as a continuous variable. The effect of common liquid contaminants on the boundary lubrication was evaluated with the liquid contaminant composition (viscosity) as the fixed-effect independent variable and COF_{BL}, τ_{hydro}, and $COF_{asymptote}$ as the dependent variables. An alpha (α) value of 0.05 was used for all analyses, based on a 95% confidence interval. Statistical analysis software, JMP 8 (SAS®, Cary, NC), was used for all statistical analyses. Only data sets with good regression fits ($R^2 > 0.8$, $n = 29$) or moderately good fits ($R^2 > 0.5$, $n = 6$) were used in this study.

3 Results and Discussion

Figure 5 shows the results of all data collection. All coefficient of friction values were found to compress to a single master curve when the coefficient of friction was plotted with respect to viscosity*speed. While not all testing conditions resulted in a decaying COF with speed over the range of 0.05–1.0 m sec^{-1}, it is expected that over a greater range of speeds, all of the conditions tested in this study would follow the trend since all data was found to compress onto a single master curve. The testing speed range of

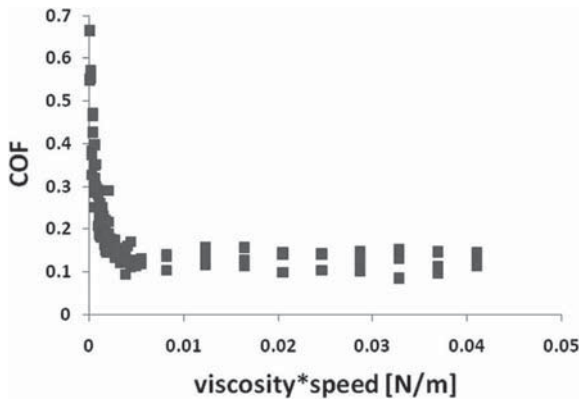

Fig. 5 Master curve of all COF data collected across all experiments plotted with respect to viscosity*speed

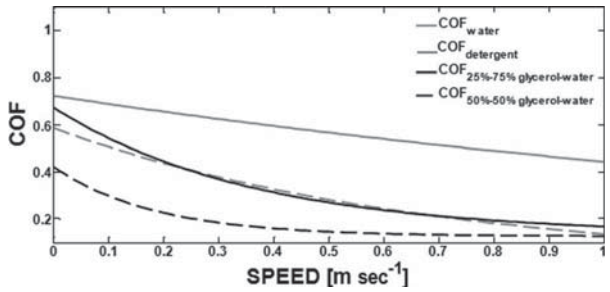

Fig. 6 Average exponential regression fits of average COF data under water, detergent, 25% glycerol-75% water, and 50% glycerol-50% water lubrication

0.05–1.0 m sec^{-1} was selected to follow the recommendations for biofidelic testing conditions [22].

Figure 6 shows the variation of the regression fit of the coefficient of friction with varying speed for various lubricants. Good exponential fits ($R^2 > 0.8$) were achieved for the fluids: 25% glycerol-75% water, detergent, and 50% glycerol-50% water. A moderately good fit ($R^2 > 0.5$) was achieved for water. Good exponential regression fits could not be made for the experimental conditions lubricated with 75% glycerol-25% water and canola oil ($R^2 < 0.5$). The COF_{BL} for canola oil and 75% glycerol-25% water was estimated by the mean coefficient of friction for the experiment. Since both lubricants' coefficient of friction values did not vary considerably with speed (i.e., the standard deviation is less than 0.05), COF_{BL} was set to the average coefficient of friction. However, since the experiments collected under 75% glycerol-25% water and canola oil lubricated conditions could not be fit with an exponential regression τ_{hydro} and $COF_{asymptote}$ could not be calculated. Therefore, these fluids were excluded from the hydrodynamic analysis, as discussed in Sec. 3.2.

3.1 Boundary Lubrication Effects. Figure 7 shows the variation of the COF_{BL} for varying lubricants. The COF_{BL} was found to be significantly affected by varying fluid lubrication as indicated by ANOVA analysis ($p_{fluid} < 0.01$). The mean boundary lubrication coefficient of friction COF_{BL} was the highest for water ($COF_{BL} = 0.69(0.04)$), followed by 25% glycerol-75% water ($COF_{BL} = 0.65(0.03)$), 1.5% detergent ($COF_{BL} = 0.58(0.03)$), 50% glycerol-50% water (0.47(0.03)), 75% glycerol-25% water ($COF_{BL} = 0.16(0.05)$), and then canola oil ($COF_{BL} = 0.10(0.02)$); see Fig. 7. Post hoc analysis revealed a significant difference between the COF_{BL} under water and 50% glycerol-50% water lubricated conditions. The COF_{BL} under the 25% glycerol-75% water lubrication was significantly higher than the COF_{BL} under 50%-50% glycerol-water lubrication. The COF_{BL} under the canola oil and the COF_{BL} under the 75% glycerol-25% water lubrication were not significantly different between the two lubrication conditions. However, the COF_{BL} of the canola oil and 75% glycerol-

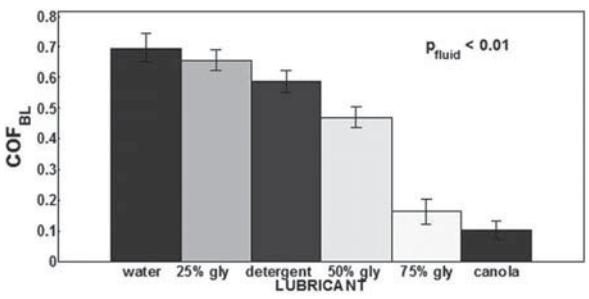

Fig. 7 Average COF_{BL} with standard deviations for water, detergent, 25% glycerol-75% water, 50% glycerol-50% water, 75% glycerol-25% water, and canola oil

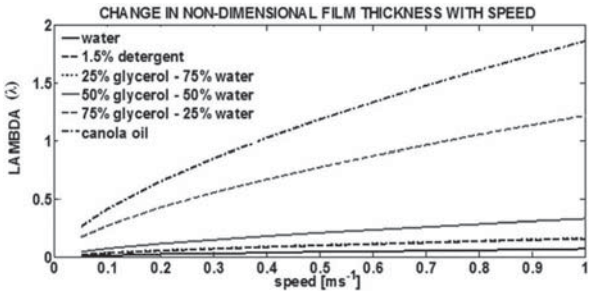

Fig. 8 Calculated nondimensional film thickness with increasing speed for water, detergent, 25% glycerol-75% water, 50% glycerol-50% water, 75% glycerol-25% water, and canola oil lubricants. (Note: the nondimensional film thickness of detergent and 25% glycerol-75% water are very close and therefore appear merged).

25% water lubricated conditions were both significantly lower when compared to the water, 25% glycerol-75% water, 1.5% detergent, and 50% glycerol-50% water lubricated conditions.

Boundary lubrication friction is significantly affected by the molecular structure of the liquid lubricant, with long chains and polar molecules providing the best liquid lubrication [27]. These long polar chains form bonds with materials creating a molecular-scale lubricating film between asperities [34]. These results are consistent with boundary lubrication theory since water is composed of the shortest molecules used in this experiment with a chemical formula of H_2O, followed by glycerol with a chemical formula of $C_3H_5(OH)_3$; canola oil has the longest chain composed of a glycerin group with long carbon chains bonded to the glycerin's hydroxyl groups [35]. It is noteworthy that, as the ratio of glycerol to water molecules increased, which would subsequently increase the average chain length, the coefficient of friction consistently decreased. The effect of the chain length of the detergent is unclear since the full composition of the industrially available detergent was not available. However, most detergents are composed of multiple components including surfactants [36], which can be used as wetting agents. Surfaces that are wetted more easily typically result in better boundary lubrication [34].

Nondimensional film thickness calculations provided insight into the lubrication regimes in which each testing shoe-floor-lubricant condition operated. Figure 8 shows the calculated nondimensional film thickness for each testing condition. The calculated nondimensional film thickness of water is lowest throughout all conditions, corresponding to the highest level of material contact and, therefore, presumably, the highest coefficient of friction under boundary conditions COF_{BL}. As predicted by the film thickness, the water lubricated contacts should never transition out of the boundary lubrication under the conditions tested. Contacts lubricated with detergent and 25% glycerol-75% water are also predicted to function only under boundary lubrication. Under 75% glycerol-25% water lubrication and canola oil lubrication the contacts are predicted to transition into mixed lubrication with increased speed. It is important to note that the nondimensional film thickness parameter λ (λ) calculated in the present investigation is contradictory with other shoe-floor-contaminant friction results, which report shoe-floor-contaminant friction functioning heavily in mixed lubrication [21,26]. The lubrication regimes were previously [21,26] identified by visual inspection. However, the calculation of the nondimensional film thickness suggests that the contact is primarily in the boundary lubrication ($\lambda < 1$), transitioning into mixed lubrication at relatively high speeds. These results suggest a speed effect within the boundary lubrication.

Additional testing was performed to determine the effect of changes in shoe material roughness on the coefficient of friction. Within the achievable range the polyurethane shoe material roughness (R_q) was 7.3 μm, 8.2 μm, and 9.3 μm. The roughness ($p = 0.3951$) and the roughness-viscosity ($p = 0.0677$) interaction did not have a significant effect on the COF_{BL}. Table 2 summarizes the results of curve fitting the collected coefficient of friction data to calculate the regression variables indicative of boundary lubrication and hydrodynamic effects. Previous researchers have found that roughness ($R_{tm} = 4.4\ \mu$m–$51.9\ \mu$m) across different shoe materials is correlated with the coefficient of friction [37,38]. Yet it is unclear if the shoe roughness or the shoe material properties caused the improved friction performance. Compared to the wide range of shoe material roughnesses that typically occur across different shoe surfaces, the range examined in this study was limited, which may explain the lack of a roughness effect. Additionally, the roughness of the less elastic material of a tribo-couple tends to have a significant influence on friction, whereas the asperities of the softer material tend to deform, resulting in a minimal influence on friction [39]. Moreover, using silicon carbide paper may not be an effective way to modify shoe roughness to achieve improved slip-performance. In this study, there was no significant difference or trend observed in the COF_{BL} due to order.

3.2 Hydrodynamic Effects. Figure 9 shows the variation of τ_{hydro} with viscosity for various lubricants. Varying the fluid contaminant significantly affected τ_{hydro}, as indicated by ANOVA analysis ($p_{fluid} < 0.001$). The fluid viscosity had a prominent effect on the hydrodynamic lubrication variable τ_{hydro}. Higher fluid viscosity resulted in less resistance to the coefficient of friction decay with increasing speed. The mean τ_{hydro} was 2.09(0.27), 0.68(0.17), 0.50(0.17), and 0.19(0.17) m sec^{-1} for water (0.52 cP), 1.5% detergent (1.8 cP), 25% glycerol-75% water (1.9 cP), and 50% glycerol-50% water (5.54 cP), respectively. When lubricated with water, the value of τ_{hydro} was very high, indicating a low sensitivity of the coefficient of friction to increasing speed, whereas τ_{hydro} was low for the 50% glycerol-50% water lubrication, indicating a low resistance of the coefficient of friction to decay with increasing speed. The effect of the fluid viscosity on the hydrodynamic lubrication is consistent with previous research [21,23,24,26]. Higher fluid viscosity resulted in a high rate of the coefficient of friction decay with increasing speed as a result of fluid pressure build-up due to the wedge effect [24,26].

The $COF_{asymptote}$ was significantly affected by the fluid contaminant composition ($p < 0.05$). The $COF_{asymptote}$ was 0.001(0.000), 0.001(0.000), 0.099(0.027), and 0.111(0.027) when the shoe-floor material was lubricated with water, 1.5% detergent, 25% glycerol-75% water, and 50% glycerol-50% water, respectively. It

Table 2 Results of regression variables (COF_{BL}, τ_{hydro}, and $COF_{asymptote}$) for varying shoe material roughness

Viscosity (composition)	Roughness	COF_{BL}	τ_{hydro} (m sec^{-1})	$COF_{asymptote}$
1.9cP (25%-75% glycerol-water)	9.3 μm	0.817 (0.049)	0.235 (0.086)	0.134 (0.033)
	8.2 μm	0.656 (0.049)	0.500 (0.086)	0.099 (0.033)
	7.3 μm	0.648 (0.049)	0.467 (0.086)	0.112 (0.033)
5.54cP (50%-50% glycerol-water)	9.3 μm	0.431 (0.049)	0.260 (0.086)	0.128 (0.033)
	8.2 μm	0.470 (0.049)	0.193 (0.086)	0.111 (0.033)
	7.3 μm	0.485 (0.054)	0.252 (0.097)	0.098 (0.037)

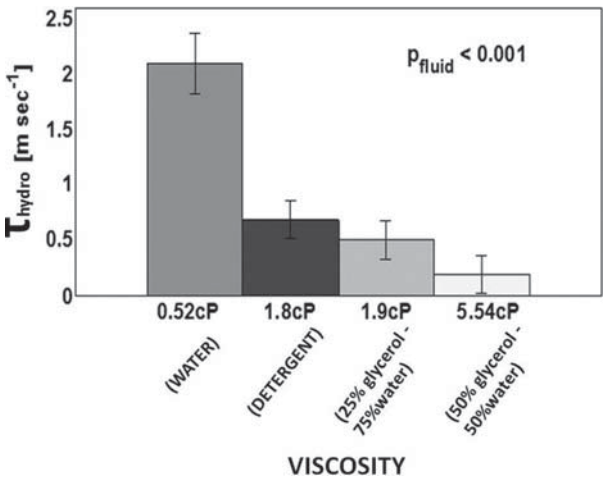

Fig. 9 Average τ_{hydro} with standard deviations for water, detergent, 25% glycerol-75% water, and 50% glycerol-50% water lubrication

should be noted that the two lowest viscosity fluids (water and 1.5% detergent), which never fully achieved their lower asymptote, had the lowest values of $COF_{asymptote}$. Because these fluids did not approach an asymptote in the tested range of speeds, the estimate of $COF_{asymptote}$ is not as reliable for water and detergent as it would be for the other fluids. Lubricated engineering materials typically have a coefficient of friction that approaches values as low as 0.001 with increasing speed [34]. In this study, along with other studies that have looked at lubricated shoe-floor friction over speed [21,26], it has been found that the values of the shoe-floor-contaminant coefficient of friction often have much higher asymptotic values, closer to 0.1, under the examined conditions. The calculations of nondimensional film thickness suggest that the shoe-floor-lubricant contact never reaches full hydrodynamic lubrication, which may explain the higher than expected asymptote. With increased speed, the contact may transition into full hydrodynamic lubrication, however, it is predicted that these speeds would be outside of the range expected for human ambulation.

Additional measurements examining the effect of achievable variations in shoe roughness under varying concentrations of glycerol identified no roughness effect (Table 2). Here, τ_{hydro} was not significantly affected by roughness ($p = 0.395$) or the viscosity-roughness ($p = 0.167$) interaction and no trends were observed. The asymptote that the COF approaches $COF_{asymptote}$ was not found to be significantly affected by fluid viscosity ($p = 0.919$), shoe material roughness ($p = 0.673$), or the combined viscosity-roughness effect ($p = 0.925$). In this study, there was no significant difference or trend observed in τ_{hydro}, or $COF_{asymptote}$ due to order.

The purpose of this study was to evaluate the effects of varying the liquid lubricant and achievable shoe material roughness on the coefficient of friction between a single shoe (polyurethane) and a single floor material (vinyl tile). Understanding the lubrication regime that is relevant to a fluid might be critical to identifying shoe and floor surfaces that should be used in environments where specific fluids are present. A combination of understanding the boundary lubrication and hydrodynamic effects may allow for the improved selection of shoe-floor combinations in expectation of the presence of a lubricant. For example, when a relatively good boundary lubricant is present, shoe and floor materials should be selected that are able to penetrate the boundary lubrication layer and make material contact. Whereas when a fluid is present that produces significant hydrodynamic effects, an improved shoe tread might be additionally necessary to reduce hydrodynamic pressures and subsequently improve frictional properties.

3.3 Limitations. A limitation of the regression model is that it did not effectively describe all experimental conditions. Not all testing conditions resulted in a decaying COF within the examined range of speeds of 0.05–1.0 m sec^{-1}. It is expected that if the testing speeds were extended, the model would have fit the water and 1.5% detergent, which is supported by the fact that all data was found to compress onto a master curve (see Fig. 5) when the COF was plotted with respect to viscosity*speed. The model may be less appropriate for long molecular length high viscous fluids including canola oil and high concentration glycerol.

Lubrication regimes were quantitatively identified by employing Hamrock and Dowson's dimensionless film thickness equation for soft-EHL. In this study, the equation was used to approximate the film thickness and identify the lubrication regime. However, a limitation of the equation is that it was derived from limited testing and, therefore, was only used to approximate shoe-floor-lubricant lubrication regimes.

3.4 Future Work. Future work would strive to improve the biofidelity of shoe-floor slip resistance testing by incorporating loading patterns which mimic gait. While friction was examined under biofidelic speeds and average pressure, factors such as loading rate, transient effects, and relative orientation are especially likely to affect the hydrodynamic lubrication in the shoe-floor interface.

Additionally, a wider range of shoe and floor materials should be examined to represent a greater number of shoe-floor combinations. This work was also limited by the narrow range of achievable variation due to mechanical abrasion with silicon carbide paper on polyurethane shoe material roughness. A greater range of shoe materials, achieved with different approaches, may result in more conclusive evidence of a shoe material roughness effect.

4 Conclusions

Important conclusions related to shoe-floor-contaminant interactions were made based on this study:

(1) This study suggests that, in some scenarios, boundary lubrication contributions may be enough to result in dangerously low available underfoot friction. The boundary coefficient of friction of shoe-floor-lubricant combinations appeared to be related to the composition of the lubricant, with longer chain, more polar, molecules resulted in the lowest boundary coefficient of friction.
(2) Based on the soft-EHL nondimensional film calculations, the shoe-floor-fluid combinations function in the boundary or mixed lubrication regions, but do not reach full hydrodynamic lubrication.

Acknowledgments

This study was funded by a research grant from the National Institute of Occupational Safety and Health (Grant No. NIOSH R01 8986-01).

Nomenclature

B = curvature regression variable
COF = available coefficient of friction (COF), measured between shoe and floor material
$COF_{asymptote}$ = COF asymptotic limit as velocity increases
COF_{BL} = y-intercept, indicative of friction as speed approaches zero and boundary lubrication affects are dominant
E' = effective elastic modulus (N m^{-2})
$\tilde{h}_{min}$ = minimum film thickness (m)
$\tilde{H}_{e,min}$ = nondimensional film thickness
k = ellipticity parameter
R_q = RMS roughness (μm)

R' = reduced radius of curature (m)
U = nondimensional speed parameter
v = velocity (m sec^{-1})
w = normal load (N)
W = nondimensional load parameter
η = viscosity (Pa s)
τ_{hydro} = resistance to COF decay with increasing speed (m sec^{-1})

References

[1] Liberty Mutual Research Institute, 2009, "The Most Disabling Workplace Injuries Cost Industry an Estimated $52 Billion."
[2] Courtney, T. K., Sorock, G. S., Manning, D. P., Collins, J. W., and Holbein-Jenny, M. A., 2001, "Occupational Slip, Trip, and Fall Related Injuries—Can the Contribution of Slipperiness be Isolated?," Ergonomics, **44**, pp. 1118–1137.
[3] National Floor Safety Institute (NFSI), 2010, http://www.nfsi.org
[4] Bureau of Labor Statistics (BLS), 2009, "Nonfatal Occupational Injuries and Illnesses Requiring Days Away From Work, 2008."
[5] Hanson, J. P., Redfern, M. S., and Mazumdar, M., 1999, "Predicting Slips and Falls Considering Required and Available Friction," Ergonomics, **42**(12), pp. 1619–1633.
[6] Burnfield, J. M., and Powers, C. M., 2006, "Prediction of Slips: An Evaluation of Utilized Coefficient of Friction and Available Slip Resistance," Ergonomics, **49**(10), pp. 982–995.
[7] Perkins, P. J., 1978, "Measurement of Slip Between the Shoe and Ground During Walking," ASTM Spec. Tech. Publ., **649**, pp. 71–87.
[8] Redfern, M. S., and DiPasquale, J., 1997, "Biomechanics of Descending Ramps," Gait and Posture, **6**(2), pp. 119–125.
[9] Strandberg, L., 1983, "On Accident Analysis and Slip-Resistance Measurement," Ergonomics, **26**, pp. 11–32.
[10] Cham, R. and Redfern, M. S., 2001, "Lower Extremity Corrective Reactions to Slip Events," J. Biomech., **34**(11), pp. 1439–1445.
[11] Redfern, M. S., and Bidanda, B., 1994, "Slip Resistance of the Shoe-Floor-Interface Under Biomechanically-Relevant Conditions," Ergonomics, **37**(3), pp. 511–524.
[12] Grönqvist, R., 1995, "Mechanisms of Friction and Assessment of Slip Resistance of New and Used Footwear Soles on Contaminated Floors," Ergonomics, **38**(2), pp. 224–241.
[13] Chang, W. R., and Matz, S., 2001, "The Slip Resistance of Common Footwear Materials Measured With Two Slipmeters," Appl. Ergon., **32**, pp. 549–558.
[14] Chang, W. R., 1998, "The Effect of Surface Roughness on Dynamic Friction Between Neolite and Quarry Tile," Safety Sci., **29**, pp. 89–105.
[15] Chang, W. R., 1999, "The Effect of Surface Roughness on the Measurement of Slip Resistance," Int. J. Ind. Ergon., **24**, pp. 229–313.
[16] Chang, W. R., Kim, I. J., Manning, D. P., and Bunterngchit, Y., 2001, "The Role of Surface Roughness in the Measurement of Slipperiness," Ergonomics, **44**(13), pp. 1200–1216.
[17] Kim, I. J., and Smith, R., 2000, "Observation of the Floor Surface Topography Changes in Pedestrian Slip Resistance Measurements," Int. J. Ind. Ergon., **26**, pp. 581–601.
[18] Gao, C., Abeysekera, J., Hirvonen, M., and Grönqvist, R., 2004, "Slip Resistant Properties of Footwear on Ice," Ergonomics, **47**(6), pp. 710–716.
[19] Li, K. W., and Chen, C. J., 2004, "The Effect of Shoe Soling Tread Groove Width on the Coefficient of Friction With Different Sole Materials, Floors, and Contaminants," Appl. Ergon., **35**(6), pp. 499–507.
[20] Li, K. W., and Chen, C. J., 2005, "Measurement of Floor Slipperiness Using Footwear Pads With Various Tread Groove Width Design," J. Chin.Inst. Ind. Eng., **22**(5), pp. 408–418.
[21] Beschorner, K. E., Redfern, M. S., Porter, W. L., and Debski, R. E., 2007, "Effects of Slip Testing Parameters on Measured Coefficient of Friction," Appl. Ergon., **38**, pp. 773–780.
[22] Chang, W. R., Grönqvist, R., Leclercq, S., Myung, R., Makkonen, L., Strandberg, L., Brungraber, R. J., Mattke, U., and Thorpe, S. C., 2001, "The Role of Friction in the Measurement of Slipperiness—Part 1: Friction Mechanisms and Definition of Test Conditions," Ergonomics, **44**(13), pp. 1217–1232.
[23] Strandberg, L., 1985, "The Effect of Conditions Underfoot on Falling and Overexertion Accidents," Ergonomics, **28**, pp. 131–147.
[24] Proctor, T. D., and Coleman, V., 1988, "Slipping, Tripping and Falling Accidents in Great Britain—Present and Future," J. Occup. Accid., **9**, pp. 269–285.
[25] Moore, D. F., 1972, "The Friction and Lubrication of Elastomers," *International Series of Monographs on Material Science and Technology*, Vol. 9, G. V. Raynor, ed., Pergamon, Oxford,.
[26] Beschorner, K., Lovell, M., Higgs, C. F., III, and Redfern, M. S., 2009, "Mixed-Lubrication of a Shoe-Floor Interface Applied to a Pin-On-Disk Apparatus," Tribol. Trans., **52**, pp. 560–568.
[27] Bhushan, B., and Zhao, Z., 1999, "Macro- and Microscale Tribological Studies of Molecularly-Thick Boundary Layer of Perfluoropolyether Lubricants for Magnetic Thin-Film Rigid Disks," J. Inf. Storage Process. Syst., **1**, pp. 1–21.
[28] Li, K. W., Chang, W. R., Leamon, T. B., and Chen, C. J., 2004, "Floor Slipperiness Measurements: Friction Coefficient, Roughness of Floors, and Subjective Perception Under Spillage Conditions," Safety Sci., **42**, pp. 547–565.
[29] Nelder, J. A., and Mead, R., 1965, "A Simplex Method for Function Minimization," Comput. J., **7**, pp. 308–313.
[30] Lagarias, J. C., Reeds, J. A., Wright, M. H., and Wright, P. E., 1998, "Convergence Properties of the Nelder-Mead Simplex Method in Low Dimensions," SIAM J. Optim., **9**(1), pp. 112–147.
[31] D'Errico, J., 2006, "MATLAB Central-File Detail-Fminsearchbnd. MathWorks-MATLAB and Simulink for Technical Computing," http://www.mathworks.com/matlabcentral/fileexchange/8277-fminsearchbnd
[32] Esfahanian, M., and Hamrock, B. J., 1991, "Fluid-Film Lubrication Regimes Revisited," Tribol. Trans., **3**(4), pp. 618–632.
[33] Hamrock, B. J., 1994, *Fundamentals of Fluid Film Lubrication*, 1st ed., McGraw-Hill, New York.
[34] Bhushan, B., 2002, *Introduction to Tribology*, John Wiley & Sons, New York.
[35] Hornback, J. M., 2006, *Organic Chemistry*, Thomson, Belmont, CA.
[36] Lai, K. Y., 2006, *Liquid Detergents*, Taylor & Francis, Boca Raton.
[37] Rowland, F. J., Jones, C., and Manning, D. P., 1996, "Surface Roughness of Footwear Soling Materials: Relevance to Slip Resistance," J. Test. Eval., **24**(6), pp. 368–376.
[38] Manning, D. P., Jones, C., Rowland, F. J., and Roff, M., 1998, "The Surface Roughness of a Rubber Soling Material Determines the Coefficient of Friction on Water-Lubricated Surfaces," J. Safety Res., **29**(4), pp. 275–283.
[39] Menezes, P. L., Kishore, S. M., Kailas, S. V., and Lovell, M. R., 2011, "Studies on Friction in Steel-Aluminum Alloy Tribo-System: Role of Surface Texture of the Softer Material," Proceedings of the STLE 2011 Annual Meeting and Exhibition, Atlanta, Georgia, Paper No. STLE2011-1005453.